Journal of
Materials Chemistry B

PAPER

View Article Online
View Journal

Cite this: DOI: 10.1039/c5tb01870f

A toolbox for controlling the properties and functionalisation of hydrazone-based supramolecular hydrogels†

Jos M. Poolman,‡[a] Chandan Maity,‡[a] Job Boekhoven,[ab] Lars van der Mee,[a] Vincent A. A. le Sage,[a] G. J. Mirjam Groenewold,[c] Sander I. van Kasteren,[c] Frank Versluis,[a] Jan H. van Esch*[a] and Rienk Eelkema*[a]

Received 9th September 2015,
Accepted 21st December 2015

DOI: 10.1039/c5tb01870f

www.rsc.org/MaterialsB

In recent years, we have developed a low molecular weight hydrogelator system that is formed *in situ* under ambient conditions through catalysed hydrazone formation between two individually non-gelating components. In this contribution, we describe a molecular toolbox based on this system which allows us to (1) investigate the limits of gel formation and fine-tuning of their bulk properties, (2) introduce multicolour fluorescent probes in an easy fashion to enable high-resolution imaging, and (3) chemically modify the supramolecular gel fibres through click and non-covalent chemistry, to expand the functionality of the resultant materials. In this paper we show preliminary applications of this toolbox, enabling covalent and non-covalent functionalisation of the gel network with proteins and multicolour imaging of hydrogel networks with embedded mammalian cells and their substructures. Overall, the results show that the toolbox allows for on demand gel network visualisation and functionalisation, enabling a wealth of applications in the areas of chemical biology and smart materials.

Introduction

Supramolecular systems consist of self-assembled structures that are held together by non-covalent interactions. By carefully balancing the strength of the individually weak interactions, relatively robust architectures can be devised, retaining the ability to respond to environmental changes such as temperature,[1] light[2] and pH.[3] In recent years, a wealth of systems capable of forming supramolecular fibres and hydrogels has been reported.[4,5] Due to the reversible nature of the bonds that hold the network together, supramolecular hydrogels find applications as biomaterials,[6] sensors[7] and host–guest systems.[8] The gelators are often derived from biological materials such as peptides,[9–12] nucleobases,[13–15] saccharides[16–18] and hybrids thereof.[19–21] Alternatively, small synthetic organic compounds have been used extensively to form hydrogels based on non-covalent interactions.[22–28] Nevertheless, it remains difficult and laborious to modulate the properties of the obtained hydrogels, as it requires complete synthesis of a new hydrogelator. Furthermore, introduction of functional groups on the fibrillar networks typically requires multi-step syntheses of functionalised monomers,[29–31] rendering gel functionalisation an inefficient process. To overcome these challenges, we present a modular hydrogelator system that spontaneously forms *in situ* by chemical bond formation between non-gelating precursors. The chemical structure and properties of the resulting materials can be easily tuned by slight modifications of the precursor molecules. These precursor molecules are synthesised in a few, straightforward steps from readily available starting materials. Moreover, by mixing in small amounts of functionalised precursors with the standard precursors, hydrogel networks are obtained that are molecularly designed to display specific functions. In all, this strategy allows for easy tuning of hydrogel properties and further modification of the fibre network.

Recently, we have developed a supramolecular hydrogelator that is formed *in situ* through hydrazone formation between water-soluble hydrazide **H1** and aldehyde **A11** under ambient conditions (Fig. 1).[32,33] Gels will form spontaneously at room temperature after mixing of the precursors, without the need for a heating step to aid dissolution of the gelator. The rate of hydrazone formation can be increased through the use of catalysts such as aniline or acid, reducing gelation times from

[a] *Advanced Soft Matter, Department of Chemical Engineering, Delft University of Technology, Julianalaan 136, 2628 BL Delft, The Netherlands. E-mail: r.eelkema@tudelft.nl, j.h.vanesch@tudelft.nl*
[b] *Institute for Advanced Study and Department of Chemistry, Technische Universität München, Lichtenbergstrasse 2A, 85748 Garching, Germany*
[c] *Leiden Institute of Chemistry and The Institute for Chemical Immunology, Leiden University, Einsteinweg 55, 2333 CC Leiden, The Netherlands*

† Electronic supplementary information (ESI) available: Synthesis, characterisation, and experimental procedures. See DOI: 10.1039/c5tb01870f

‡ These authors contributed equally.

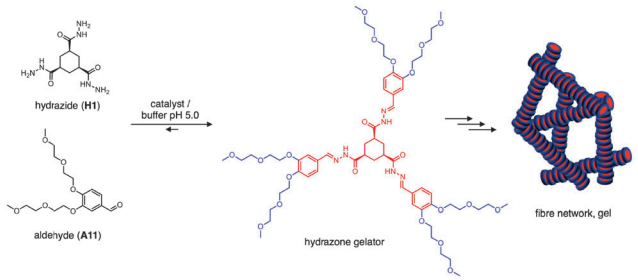

Fig. 1 Schematic representation of catalysed gel formation. Soluble, non-gelating starting components **H1** and **A11** react to give a self-assembling hydrogelator molecule, which assembles into fibres and finally a network, gelling the solvent.

hours to minutes. Upon reaching a critical minimum concentration, the hydrazone gelator self-assembles into fibres, which in due course form a network capable of retaining water. The use of catalysis supplies us with a handle through which the rate of formation and mechanical properties of the gel network can be controlled.[33] Additionally, we have shown that through the catalyst the spatial distribution of gel formation can be controlled, using micro-patterned catalytic surfaces[34] or a light triggered catalyst.[35] In this contribution we present a molecular toolbox which is aimed at: (1) investigating the molecular constraints of gel formation, (2) covalently functionalising the network with a variety of fluorescent probes and (3) the integration of reactive groups in the hydrogel network, allowing for further modification of the gel fibres (Fig. 2). Our approach enables easy tuning of the physical properties of the gel network and its further functionalisation. We accomplish this either using derivatives of the aldehyde and hydrazide precursors as the majority components in the gelation mixture, or by mixing in small amounts of functionalised derivatives of the benzaldehyde precursor with the standard aldehyde precursor **A11**. This makes our gel system highly versatile, enabling the incorporation of a wide variety of benzaldehyde-derived functional compounds into the gel network. Additionally, the synthesis of these derivatives is generally straightforward and can be achieved in a few steps from commonly available precursors.

Experimental section

Synthesis

Detailed synthetic procedures and characterisation are found in the ESI.†

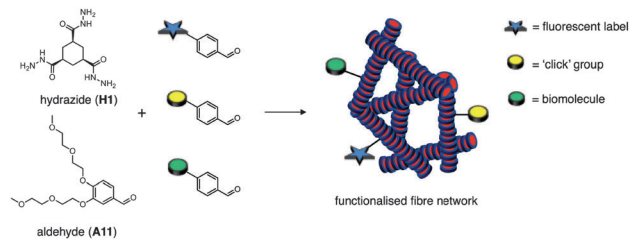

Fig. 2 Concept of functionalised gel fibre network formation *via* partial replacement of the original aldehyde (**A11**) by a functionalised aldehyde creating a gel with tailored functionalities.

Critical gelation concentration experiments

Gels were formed by preparing stock solutions of the aldehyde (240 mM) and hydrazide (40 mM) in 100 mM sodium phosphate buffer (Na_2HPO_4/NaH_2PO_4, pH 5.0). Appropriate amounts of the stock solutions were mixed and vortexed vigorously for three seconds. The mixed samples were allowed to gel overnight and gelation was checked using the inverted vial test. The critical gel concentration (CGC) is expressed as the initial concentration (in mM) of the hydrazide precursor in the mixture and defined as the point between the lowest concentration at which gels were formed and the highest concentration at which the solvent cannot be supported.

Confocal laser scanning microscopy

Stock solution of **H1**, **A11**, functionalised aldehydes (**A14–A23**, **A25**) and reactive compounds (azide-fluor 545, FITC-SH, Fluor 488-alkyne, Cy5-labelled azide-ovalbumin and fluorescein labelled Concanavalin A) were prepared in phosphate buffer of pH 5.0 (see ESI† for details). Gel samples were prepared by mixing an appropriate amount of stock solutions of **H1**, **A11** and the functionalised aldehyde. The mixture was immediately deposited into a polydimethylsiloxane cuvette or an imaging chamber (diameter × thickness = 20 mm × 0.6 mm), closed off with a glass cover slide and was allowed to stand overnight. Confocal laser scanning micrographs were obtained in the fluorescence mode on a Zeiss LSM 700. The laser beam was focused on a 40× oil immersion objective and the sensitivity of detectors and filters was adjusted accordingly to obtain the maximum signal to noise ratio. CLSM micrographs (Fig. 7 and ESI†) were recorded using the same settings (apart from the excitation wavelength) to allow comparison of the fluorescence intensity for analysis purposes.

Results and discussion

In a first study, we examined the influence of the molecular design of the precursors on gelation behaviour. To do so, we synthesised a small library of aldehyde and hydrazide derivatives, and tested all possible combinations for their gelation behaviour in a simple mixing + reaction experiment (Fig. 3 and Table 1). The benzaldehyde derivatives were functionalised with one or two ethylene glycol (EG) chains of varying length (Fig. 3),

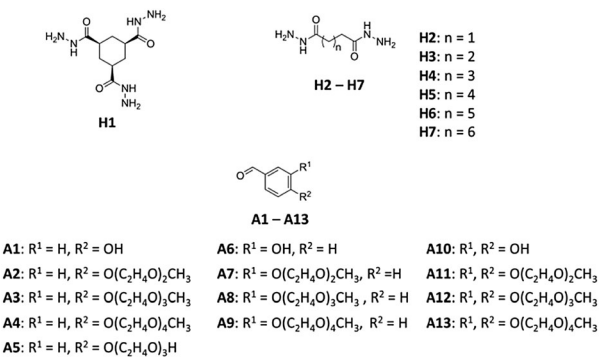

Fig. 3 Molecular structures of the hydrazide and aldehyde derivatives.

Table 1 Critical gel concentration (CGC) tests with hydrazide and aldehyde derivatives in a pH 5 sodium phosphate buffer under ambient conditions. The tests were performed by mixing the appropriate amount of hydrazide and aldehyde precursors in a sample vial and allowing the samples to stand overnight. Results after inverting the vial were classified into precipitation (P), homogeneous solution (S), opaque gel (G) and weak gel (WG), which is a gel which is not capable of supporting its own weight for >30 seconds. The given numbers are CGC values in mM, where CGC is defined as the minimum concentration of the hydrazide precursor to form a gel that withstands gravity when turned upside down

		benzaldehydes												
		para-substitution					meta				meta, para			
		A1	A2	A3	A4	A5	A6	A7	A8	A9	A10	A11	A12	A13
hydrazides: tris	H1	P	G 8	G 3.5	G 11	G 13	P	G 5.5	P	G 16	P	G 4.5	S	S
hydrazides: bis-hydrazides	H2	P	G 25	WG >25	G 25	WG >25	P	P	P	P	P	S	S	S
	H3	P	P	P	P	P	P	P	P	P	P	S	S	S
	H4	P	G 17.5	G 25	G 20	WG >25	P	P	P	P	P	S	S	S
	H5	P	P	P	P	P	P	P	P	P	P	S	S	S
	H6	P	G 14.5	P	WG >25	P	P	P	P	P	P	P	S	S
	H7	P	P	P	P	P	P	P	P	P	P	P	S	S

which increases the water solubility of the compounds due to the hydrophilic nature of EG and possibly prevents precipitation of the corresponding hydrazone through favourable interactions between the supramolecular fibres and the solvent.[36] These functions of the EG chains are assumed to be of paramount importance for the self-assembly of the hydrazone materials into fibres and subsequent gelation. The hydrazide series contained a trishydrazide (**H1**) and six bishydrazide (**H2–H7**) compounds, with a varying spacer length between the two hydrazide moieties, in the range of 2–7 carbon atoms. The hydrazides (**H1–H7**) were either commercially available or easily synthesised in one step from their corresponding methyl esters in quantitative yield without any purification steps. The aldehyde derivatives (**A2–A4**, **A7–A9**, and **A11–A13**) were synthesised in good yield (78–99%) from the corresponding hydroxybenzaldehydes (**A1**, **A6** or **A10**) by reaction with the relevant tosylated ethylene glycol monomethyl ether. Compound **A5** was synthesised in a single step by reacting **A1** and 2-[2-(2-chloroethoxy)ethoxy]ethanol.

Critical gel concentration (CGC) tests were performed to investigate the influence of the molecular design of the starting aldehydes and hydrazides on the gelation behaviour of the resulting hydrazone products. In a typical experiment, the aldehyde and hydrazide derivatives were dissolved separately in a phosphate buffer of pH 5. Whereas the starting materials did not self-assemble under these conditions, mixing the two solutions resulted in conversion to the expected gelating hydrazone products.[32] To promote the full conversion of hydrazides into hydrazones, two equivalents of aldehyde were added for each hydrazide group. Evaluation of the CGC tests was performed by the inverted vial test after the solution had been allowed to stand overnight at room temperature.

Mixing hydrazide **H1** with non-EG-modified benzaldehyde derivatives (**A1**, **A6**, **A10**) yielded precipitated hydrazone materials instead of gelation. In contrast, benzaldehyde derivatives bearing more than four EG monomers (**A12**, **A13**) yielded too water-soluble hydrazone materials, maintaining clear solutions after reaction (Table 1). In between these two extremes, however, opaque gels with a water content of up to 99.5% (w/w) were obtained from benzaldehyde derivatives modified with 2 to 4 EG, pointing towards a balance between the crystallisation and solubilisation processes. *para*-Functionalised benzaldehyde derivatives (**A2–A5**) provided stable hydrogels. The optimum gelation efficiency (*i.e.* lowest CGC, 3.5 mM) was obtained using three EG units (**A3**), whereas benzaldehyde derivatives with shorter (**A2**) and longer EG (**A4**, **A5**) needed higher gelator concentrations (8, 11 and 13 mM respectively). In contrast, *meta*-functionalised benzaldehyde derivatives (**A7–A9**) showed poor solubility in water compared to their *para*-functionalised counterparts. This effect is presumably due to higher aromatic surface exposure towards the aqueous environment. Reacting **H1** with either **A7** or **A9** (containing 2 and 4 EG, resp.) yielded gels at the respective concentrations of 5.5 mM and 16 mM, whereas **A8** with 3 EG provided a hydrazone material that precipitated in the form of oil droplets at the bottom of the vial. The *meta*- and *para*-functionalised aldehyde (**A11**) with four EG provided a hydrogel with a CGC of 4.5 mM. Furthermore, a benzaldehyde derivative with a terminal hydroxy group on the EG (**A5**) gelated less efficiently than the corresponding derivative with a methyl terminated chain (**A3**).

Mixing benzaldehyde derivatives with dihydrazide compounds (**H2–H7**) generally afforded gels at higher minimum gelation concentrations (14.5–25 mM) than for **H1** (3.5–16 mM). Also, the range of benzaldehyde derivatives that would yield a gel was narrower (Table 1). Remarkably, dihydrazides with a spacer composed of an even number of carbon atoms (**H2**, **H4**, and **H6**) yielded hydrogels, whereas precipitation was observed for the dihydrazides with an odd numbered carbon spacer (**H3**, **H5**, and **H7**). Upon reaction with *meta*-functionalised benzaldehydes (**A7–A9**), dihydrazides with an even carbon atom spacer yielded crystalline precipitates whereas hydrazone materials with odd carbon atom spacer phase separated in the form of oil droplets. Increasing the length of the carbon atom spacer and thereby decreasing hydrophobicity has a favourable effect on the gelation of the formed hydrazones as lower gelator concentrations are observed with increasing chain length, eventually limited by the solubility of the hydrazide derivative.

For selected samples, we determined the stiffness of the obtained gels using oscillatory rheology (Fig. 4a). The elastic modulus G' varied over three orders of magnitude, between 45 Pa (**H2** + **A3**) and 1.2×10^5 Pa (**H1** + **A11**). In general, an inverse relationship between the observed elastic modulus and the CGC can be observed (Fig. 4b), showing that a lower CGC in general predicts a higher elastic modulus of the obtained material. As all samples were measured at a fixed 20 mM concentration, this general trend partly originates from the higher fibre density for lower-CGC samples, leading to higher G'. Fig. 4b also shows a bifurcation in the CGC-G' dependence, with a steeper dependence for **H1** derived gels compared to those derived from **H2–6**. Such a difference in behaviour may point to a different mode of gelation.

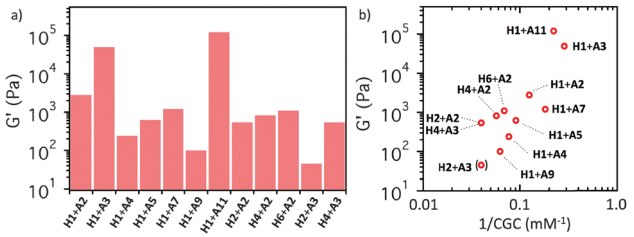

Fig. 4 Rheological data of selected hydrogels. (a) Elastic moduli (G'), measured for 20 mM gels, 20 mM of any hydrazide derivative, 120 mM of aldehyde derivative (for **H1**) or 80 mM of aldehyde derivative (for **H2–6**). (b) A plot of G' *versus* the inverse of the CGC. For each point, the corresponding gel mixture is indicated. The **H2** + **A3** data point is indicated in parentheses, as its CGC was determined at >25 mM (see Table 1).

To get some insight into the morphology of these gels, we collected TEM micrographs for the **H1** + **A2**, **H1** + **A7**, **H1** + **A11** and **H6** + **A2** gels. All **H1** derived gels gave dense fibre networks consisting of fibres with diameters <10 nm. The **H6** + **A2** gel, however, showed plate-type structures with dimensions in the micrometre range (see the ESI†). This change in morphology may account for the marked difference in both CGC and the relationship between CGC and G', when compared to **H1** derived gels.

As shown above, our supramolecular gel system enables the tuning of gelation properties such as CGC, elastic modulus or network morphology by changing the aldehyde or hydrazide structure. Next, we made use of this modularity to incorporate chemical labels in the structure. For these experiments, we used the well-characterised **H1–A11** system[32,33] as a common gelator. In a first example, we replaced small fractions of the reacting aldehyde derivatives with aldehyde-derived fluorophores (Fig. 5). As we observed earlier that the trishydrazide (**H1**) showed gelation after reaction with a wide range of aldehyde derivatives (Table 1), we anticipated that small percentages of other aldehyde derivatives can be incorporated into the supramolecular gel network without hindering gel formation. Using fluorescently labelled aldehyde derivatives allows for imaging of the structure of the supramolecular network using confocal laser scanning microscopy (CLSM). We used various fluorescent probes, with different excitation wavelengths. This strategy increases our flexibility with respect to future applications of our hydrogel system, for instance as scaffolds for 3D cell culturing. There, typically, imaging of cell membranes or nuclei will be performed with the aid of a fluorescent probe, illustrating the need for flexibility in the choice of probe to simultaneously image the hydrogel network structure. Therefore, we synthesised fluorescent styryl, coumarin, fluorescein, rhodamine and cyanine derivatives that contain an aldehyde functionality (Fig. 5).

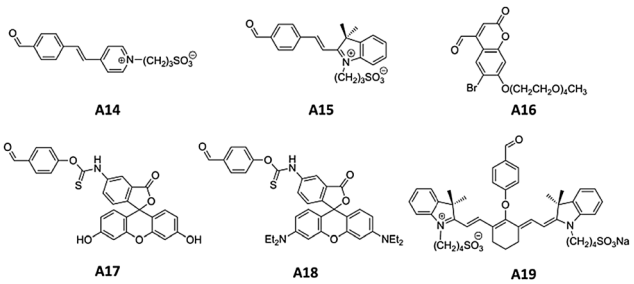

Fig. 5 Molecular structures of fluorophore labelled aldehydes.

Styryl labelled aldehydes (**A14**, **A15**) were synthesised from terephthalaldehyde *via* a condensation reaction with the corresponding pyridinium (yielding **A14**) and indolium (yielding **A15**) sulfonate salts. Coumarin labelled aldehyde (**A16**) was synthesised *via* allylic oxidation of the corresponding methyl derivative. Fluorescein (**A17**), rhodamine (**A18**) and cyanine (**A19**) labelled aldehydes were acquired *via* reaction of 4-hydroxybenzaldehyde with fluorescein isothiocyanate, rhodamine B isothiocyanate and IR-783, respectively. After obtaining compounds **A14–A19**, gels were formed using hydrazide **H1** and aldehyde **A11**, incorporating 0.1 mol% (with respect to aldehyde **A11**) of the fluorescently labelled aldehyde. Subsequently, the structure of the resulting gel networks were analysed using CLSM (Fig. 6). In all cases, a branched network of fibre bundles is observed, showing that the fluorescently labelled aldehydes are incorporated into the gel network, without observably disturbing fibre formation. Furthermore, exciting the various probes was achieved using lasers with different wavelengths, depending on their absorption characteristics. The styryl (**A14**, **A15**) and coumarin (**A16**) derivatives were excited at 405 nm, whereas the fluorescein (**A17**), rhodamine (**A18**), and cyanine derivatives (**A19**) required 488, 543 and 633 nm lasers, respectively. Therefore, this toolbox of fluorescently labelled aldehydes should allow for the introduction of other species with orthogonal fluorescent labels into our gel system (*e.g.* cells).

Encouraged by the above results, we set out to demonstrate the use of our fluorescent gel network in combination with fluorescently tagged mammalian cells (mouse brain derived astrocytes). In a preliminary set of experiments, we first fluorescently

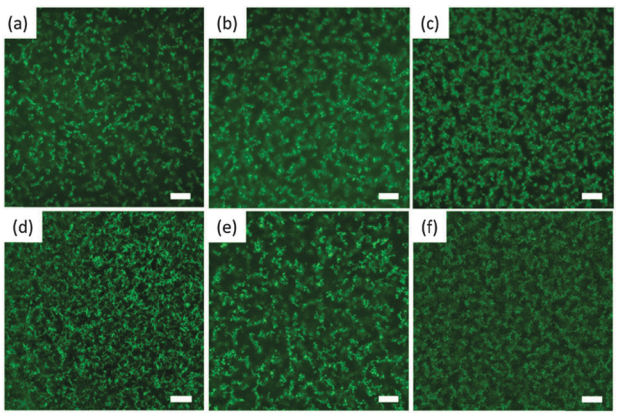

Fig. 6 Confocal laser scanning fluorescence micrographs (CLSM) of gel networks made using various aldehyde-derived fluorescent probes (scale bar = 20 μm): (a) styryl-pyridinium derivative (**A14**), (b) styryl-indolium derivative (**A15**), (c) coumarin derivative (**A16**), (d) fluorescein derivative (**A17**), (e) rhodamine derivative (**A18**), and (f) cyanine derivative (**A19**). General conditions: [**H1**] : [**A11**] = 5 : 30 mM, a 1 : 2 ratio of hydrazide to aldehyde functional groups at pH 5, fluorophore labelled aldehyde (30 μM, 0.1 mol% with respect to **A11**).

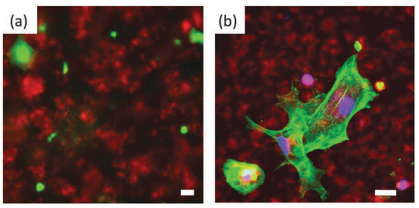

Fig. 7 Merged confocal laser scanning micrographs (CLSM) of astrocytes embedded in a gel network made of **H1**, **A11** and **A18** (scale bar = 20 μm). (a) The green channel shows calcein-AM-stained cells ($\lambda_{exc.}$ = 488 nm) and the red channel gel fibres ($\lambda_{exc.}$ = 543 nm), (b) nuclei are shown in blue ($\lambda_{exc.}$ = 404 nm), the green channel are actin filaments ($\lambda_{exc.}$ = 488 nm) and the red channel represents gel fibres ($\lambda_{exc.}$ = 543 nm). Concentrations: [**H1**] : [**A11**] = 10 : 60 mM, [**A18**] = 30 μM.

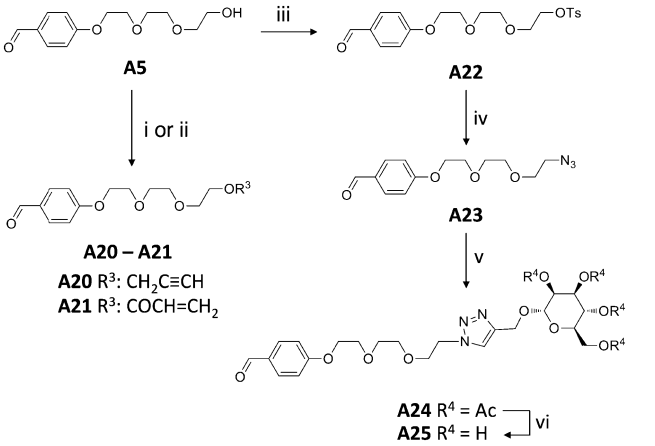

Fig. 8 Synthesis of aldehyde derivatives with functional groups for fibre-modification. Reagents and conditions: (i) Br–$CH_2C{\equiv}CH$, NaH, THF, rt; (ii) $ClCOCH{=}CH_2$, Et_3N, CH_2Cl_2, 0 °C → rt; (iii) Ts-Cl, Et_3N, CH_2Cl_2, rt; (iv) NaN_3, DMF, Δ; (v) 2,3,4,6-tetraacetylpropargyl-α-mannoside, CuI, Et_3N, CH_2Cl_2, rt; (vi) NaOMe, MeOH, rt.

labelled these cells with calcein-AM, a green marker for viable cells. These cells were combined with our gel network that was functionalized with the red fluorescent **A18** dye. Using fluorescence microscopy, we imaged the cells in the green channel and the fibres in the red channel and found the cells embedded in the gel network (Fig. 7a). Secondly, we used the same astrocytes, but in this case the cells were fixed and permeabilised. Subsequently, their actin filaments were labelled with a fluorescein-conjugated phalloidin (green) and their nuclei with DAPI (blue). Finally, the gel network with the red fluorescent **A18** dye was added to demonstrate the orthogonality of the fluorescent dyes. Using confocal microscopy, we imaged the system and found the nucleus, actin filaments and gel network individually marked blue, green and red, respectively (Fig. 7b).

We further expanded the toolbox of functional precursors by synthesising aldehyde derivatives with reactive groups, allowing for modification of the fibre network, either through the formation of permanent covalent bonds *via* click chemistry,[37,38] or by non-covalent interactions with biomolecules. Three aldehyde derivatives were synthesised containing functionalities for either Michael addition or alkyne–azide click chemistry, and an α-mannose derived aldehyde was synthesised to decorate the fibres with sugar groups, and to show non-covalent binding of the lectin Concanavalin A (**ConA**) to the gel fibres.[39] The aldehydes with reactive groups were synthesised from 4-(2-(2-(2-hydroxyethoxy)ethoxy)ethoxy)benzaldehyde (**A5**) (Fig. 8). Alkyne (**A20**) and enone (**A21**) labelled aldehyde derivatives were synthesised *via* nucleophilic substitution of **A5** to propagyl bromide and acryloyl chloride respectively. Alternatively, the hydroxy group of **A5** was converted to a tosylate group (**A22**) *via* the treatment with tosyl chloride. An azide derivative (**A23**) was obtained from **A22** *via* nucleophilic substitution with the azide ion. A Cu-catalysed cycloaddition of **A22** with the alkyne-functionalised 2,3,4,6-tetraacetylpropargyl-α-mannoside provided the acetate-protected mannose-benzaldehyde conjugate **A24**, which afforded the mannose derivative **A25** *via* removal of the acetate groups.

Incorporation of alkyne bearing aldehyde **A20** into the network allows for covalent addition of azide compounds, whereas the azide containing compound **A23** enables the Cu mediated azide alkyne Huisgen cycloaddition with any alkyne derivative. Incorporation of alkene **A21** allows for Michael addition of thiols. Gel network functionalisation with **A20** and **A23** was attempted by forming gels with **H1** and **A11**, mixed with **A20** or **A23** (0.3 mol%, with respect to **A11**). Styryl labelled aldehyde **A15** (0.05 mol%) was used for imaging the gel network (Fig. 9). During gel formation, azide functionalised rhodamine (azide-fluor 545) was added to the gelation mixture containing acetylene derivatised aldehyde **A20**, whereas acetylene functionalised rhodamine (fluor 488-alkyne) was added to the gelation mixture containing azido-aldehyde **A23**. CuI was added to catalyse the click reaction. After gelation, confocal imaging showed colocalisation of the rhodamine fluorescence with the styryl fluorescence of the gel network (Fig. 9). These findings clearly demonstrate successful functionalisation of styryl stained fibres with a rhodamine

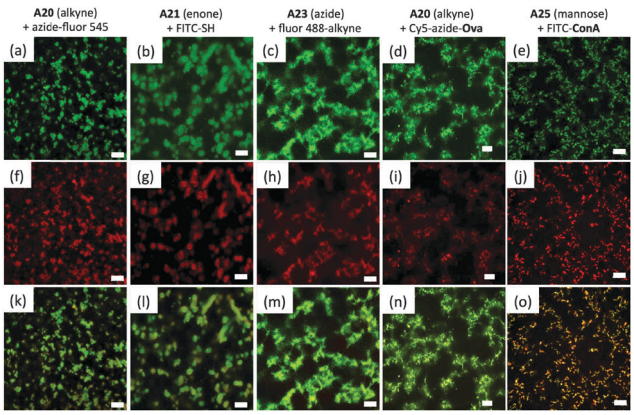

Fig. 9 Confocal laser scanning fluorescence micrographs of functionalised gel networks (scale bar = 20 μm) in the presence of **A20** and azide-fluor 545 (a, f and k), **A21** and FITC-SH (b, g and l), **A23** and fluor 488-alkyne (c, h and m), **A20** and Cy5-azide-**Ova** (d, i and n), and **A25** with FITC-**ConA** (e, j and o): (a–d) $\lambda_{exc.}$ = 405 nm (exciting the **A15** styryl dye), (e and g) $\lambda_{exc.}$ = 488 nm (exciting FITC), (f) $\lambda_{exc.}$ = 543 nm (exciting fluor-545), (h) $\lambda_{exc.}$ = 488 nm (exciting fluor-488), (i) $\lambda_{exc.}$ = 633 nm (exciting Cy5), (j) $\lambda_{exc.}$ = 543 nm (exciting **A18** rhodamine), (k) $\lambda_{exc.}$ = 405 & 543 nm, (l) $\lambda_{exc.}$ = 405 & 488 nm, (m) $\lambda_{exc.}$ = 405 & 488 nm, (n) $\lambda_{exc.}$ = 405 & 633 nm and (o) $\lambda_{exc.}$ = 488 & 543 nm. For general conditions, see the ESI.†

dye using click chemistry. Similar to the Cu-catalysed click reaction to functionalise azide or alkyne derived gelators, a thia-Michael click reaction was performed during gelation to generate functionalised gel fibres. During gelation, 0.5 mol% enone-derived **A21** (with respect to **A11**) and fluorescein labelled thiol (FITC-SH) were added to the mixture. The gel network was visualised using incorporated **A15** and again, the fluorescence colocalisation of fluorescein and **A15** indicated functionalisation of the fibres using the click reaction (Fig. 9).

To determine the scope of the approach, we also applied this methodology to functionalise the gel network with various biomolecules. We first attempted the direct attachment of a protein to the gel by performing a click-reaction of a model antigenic protein (ovalbumin,[40] **Ova**), with the gel matrix. **Ova** is the most commonly used model antigen in immune assays. In future, ovalbumin-conjugation to the gel matrix would allow the study of any immunogenicity of these gel matrices using standard T-cell assays.[41] The protein was functionalised with azides by expression in a methionine auxotrophic strain of *E. coli* to replace all methionines with azidohomoalanines[42–44] without affecting the structure and function of the protein.[45] The protein was further functionalised with Cy5 dyes through lysine modification, to allow facile visualisation using confocal microscopy. By adding the azide-**Ova** to a gelation mixture containing Cu(I) and the acetylene-aldehyde **A20**, as well as the styryl-aldehyde probe **A15** for visualisation of the fibre network, an **Ova**-functionalised gel was obtained. CLSM showed extensive colocalisation of the styryl and Cy5 dyes indicating binding of **Ova** to the fibres (Fig. 9d, i and n). Controls with wild-type **Ova** (without azide tag) or by leaving out the acetylene-aldehyde from the gelation mixture showed a severely weakened intensity of the fluorescence intensity of the Cy5 probe, as well as a diminished colocalisation with the styryl probe, indicating a lack of binding to the fibres (see Fig. S7, ESI†). As a second class of biomolecules, we functionalised the fibres with sugar groups. To demonstrate that aldehyde **A25** allows for the functionalisation of the gel network with mannose moieties, gels were formed using trishydrazide **H1** and aldehyde **A11**, mixed with 1 mol% (with respect to aldehyde **A11**) mannose derivative **A25**. Furthermore, rhodamine labelled aldehyde **A18** was incorporated (0.02 mol%) to enable imaging of the gel network using CLSM (Fig. 9). During gel formation, a fluorescein derivative of the lectin Concanavalin A (**ConA**) was added, which was expected to bind specifically to the mannose present in the gel fibres.[30] Confocal imaging showed that the **ConA** fluorescence (Fig. 9) displayed extensive colocalisation with the rhodamine fluorescence of the gel network, indicating functionalisation of the fibre network with mannose and selective binding to the lectin. Control experiments, in which the gel sample was prepared without addition of the functional aldehydes, did not show fluorescence colocalization by CLSM from two different fluorophores used in the sample (see Fig. S6, ESI†), thus ruling out the possibility of non-specific binding of the added functional groups to the gel fibres. Using TEM, we investigated the impact of the incorporation of a fluorophore (**A18**) or the **A25–ConA** pair on the morphology of **H1** + **A11** fibres. In both cases, no significant changes in morphology or fibre diameter were observed (see the ESI†). These experiments show that it is possible to functionalise the fibres with aldehyde-derived sugar groups, and that such functional groups can subsequently be used for non-covalent binding to other (protein) biomolecules. Overall, these examples clearly illustrate that modification of the gel network can be achieved using these functional aldehydes and shows the utility of the various fluorescently labelled aldehydes that we developed.

Conclusions

In this paper, we present a molecular toolbox for controlling the gelation properties and functionalisation of hydrazone-derived supramolecular gels. These gels are made in the gelation medium under ambient conditions by hydrazone formation between simple, non-gelating building blocks. First we show that by varying the chemical structure and hydrophilicity of the individually non-gelating starting components the gelation behaviour of the resulting hydrazone compounds can be controlled. Next, we show how replacing a small part of the regular aldehyde by an aldehyde carrying a functional tag can be used to introduce functional groups in the supramolecular gels. Introduction of various fluorescent probes in the gel network was performed using fluorescently labelled aldehydes. Confocal imaging showed that these fluorescent probes can be used for imaging of the gel network at a wide range of excitation wavelengths. This enables multicolour imaging which allows for the visualisation of hydrogel networks in conjunction with cells and cellular substructures. Next, aldehyde derivatives with various functional groups were synthesised, allowing for facile covalent and non-covalent modification of the supramolecular fibres. In particular, various labels for click-chemistry were introduced, as well as a sugar-derived functional group capable of non-covalent binding to a lectin protein. The click groups were used for *in situ* connection to fluorescent labels or protein tags. The results show that the gel system can be modified on demand without hindering gel formation, enabling applications in the area of smart materials and chemical biology. Moreover, the modular nature of the gel formation and the facile synthesis of the various building blocks make this a straightforward method to construct complex functional materials from simple building blocks, eliminating the need for long and difficult synthetic procedures.

Acknowledgements

We thank the Netherlands Organization for Scientific Research (NWO VENI and VIDI grants to R. E., ECHO grant to J. P., R. E., J. H. v. E.) and the European Research Council (ERC Starting Grant #639005 to S. I. v. K.) for funding.

References

1 P. Cordier, F. Tournilhac, C. Soulie-Ziakovic and L. Leibler, *Nature*, 2008, **451**, 977–980.
2 Y. Zhao, *Macromolecules*, 2012, **45**, 3647–3657.

3 H. Frisch and P. Besenius, *Macromol. Rapid Commun.*, 2015, **36**, 346–363.
4 L. E. Buerkle and S. J. Rowan, *Chem. Soc. Rev.*, 2012, **41**, 6089–6102.
5 X. Du, J. Zhou and B. Xu, *Chem. – Asian J.*, 2014, **9**, 1446–1472.
6 S. I. Stupp, *Nano Lett.*, 2010, **10**, 4783–4786.
7 D. Bardelang, M. B. Zaman, I. L. Moudrakovski, S. Pawsey, J. C. Margeson, D. Wang, X. Wu, J. A. Ripmeester, C. I. Ratcliffe and K. Yu, *Adv. Mater.*, 2008, **20**, 4517–4520.
8 S. Dong, B. Zheng, F. Wang and F. Huang, *Acc. Chem. Res.*, 2014, **47**, 1982–1994.
9 P. A. Korevaar, C. J. Newcomb, E. W. Meijer and S. I. Stupp, *J. Am. Chem. Soc.*, 2014, **136**, 8540–8543.
10 J. Li, Y. Gao, Y. Kuang, J. Shi, X. Du, J. Zhou, H. Wang, Z. Yang and B. Xu, *J. Am. Chem. Soc.*, 2013, **135**, 9907–9914.
11 J. Li, Y. Kuang, Y. Gao, X. Du, J. Shi and B. Xu, *J. Am. Chem. Soc.*, 2013, **135**, 542–545.
12 P. W. J. M. Frederix, G. G. Scott, Y. M. Abul-Haija, D. Kalafatovic, C. G. Pappas, N. Javid, N. T. Hunt, R. V. Ulijn and T. Tuttle, *Nat. Chem.*, 2015, **7**, 30–37.
13 J. Arigon, C. A. H. Prata, M. W. Grinstaff and P. Barthelemy, *Bioconjugate Chem.*, 2005, **16**, 864–872.
14 N. Sreenivasachary and J. M. Lehn, *Proc. Natl. Acad. Sci. U. S. A.*, 2005, **102**, 5938–5943.
15 S. M. Park and B. H. Kim, *Soft Matter*, 2008, **4**, 1995–1997.
16 S. Matsumoto, S. Yamaguchi, S. Ueno, H. Komatsu, M. Ikeda, K. Ishizuka, Y. Iko, K. V. Tabata, H. Aoki, S. Ito, H. Noji and I. Hamachi, *Chem. – Eur. J.*, 2008, **14**, 3977–3986.
17 P. K. Vemula, J. Li and G. John, *J. Am. Chem. Soc.*, 2006, **128**, 8932–8938.
18 G. Wang, S. Cheuk, H. Yang, N. Goyal, P. V. N. Reddy and B. Hopkinson, *Langmuir*, 2009, **25**, 8696–8705.
19 X. Du, J. Li, Y. Gao, Y. Kuang and B. Xu, *Chem. Commun.*, 2012, **48**, 2098–2100.
20 X. Li, Y. Kuang, H.-C. Lin, Y. Gao, J. Shi and B. Xu, *Angew. Chem., Int. Ed.*, 2011, **50**, 9365–9369.
21 Z. Yang, Y. Kuang, X. Li, N. Zhou, Y. Zhang and B. Xu, *Chem. Commun.*, 2012, **48**, 9257–9259.
22 J. Zhou, X. Du, Y. Gao, J. Shi and B. Xu, *J. Am. Chem. Soc.*, 2014, **136**, 2970–2973.
23 M. M. C. Bastings, S. Koudstaal, R. E. Kieltyka, Y. Nakano, A. C. H. Pape, D. A. M. Feyen, F. J. van Slochteren, P. A. Doevendans, J. P. G. Sluijter, E. W. Meijer, S. A. J. Chamuleau and P. Y. W. Dankers, *Adv. Healthcare Mater.*, 2014, **3**, 70–78.
24 J. Leckie, A. Hope, M. Hughes, S. Debnath, S. Fleming, A. W. Wark, R. V. Ulijn and M. D. Haw, *ACS Nano*, 2014, **8**, 9580–9589.
25 Y. Kuang, J. Shi, J. Li, D. Yuan, K. A. Alberti, Q. Xu and B. Xu, *Angew. Chem., Int. Ed.*, 2014, **53**, 8104–8107.
26 L. Albertazzi, D. van der Zwaag, C. M. A. Leenders, R. Fitzner, R. W. van der Hofstad and E. W. Meijer, *Science*, 2014, **344**, 491–495.
27 K. J. C. van Bommel, C. van der Pol, I. Muizebelt, A. Friggeri, A. Heeres, A. Meetsma, B. L. Feringa and J. van Esch, *Angew. Chem., Int. Ed.*, 2004, **43**, 1663–1667.
28 M. Guo, L. M. Pitet, H. M. Wyss, M. Vos, P. Y. W. Dankers and E. W. Meijer, *J. Am. Chem. Soc.*, 2014, **136**, 6969–6977.
29 J. D. Hartgerink, E. Beniash and S. I. Stupp, *Proc. Natl. Acad. Sci. U. S. A.*, 2002, **99**, 5133–5138.
30 M. K. Mueller and L. Brunsveld, *Angew. Chem., Int. Ed.*, 2009, **48**, 2921–2924.
31 B. S. Kim, D. J. Hong, J. Bae and M. Lee, *J. Am. Chem. Soc.*, 2005, **127**, 16333–16337.
32 J. Boekhoven, J. M. Poolman, C. Maity, F. Li, L. van der Mee, C. B. Minkenberg, E. Mendes, J. H. van Esch and R. Eelkema, *Nat. Chem.*, 2013, **5**, 433–437.
33 (*a*) J. M. Poolman, J. Boekhoven, A. Besselink, A. G. L. Olive, J. H. van Esch and R. Eelkema, *Nat. Protoc.*, 2014, **9**, 977–988; (*b*) R. Eelkema and J. H. van Esch, *Org. Biomol. Chem.*, 2014, **12**, 6292–6296.
34 A. G. L. Olive, N. H. Abdullah, I. Ziemecka, E. Mendes, R. Eelkema and J. H. van Esch, *Angew. Chem., Int. Ed.*, 2014, **53**, 4132–4136.
35 C. Maity, W. E. Hendriksen, J. H. van Esch and R. Eelkema, *Angew. Chem., Int. Ed.*, 2015, **54**, 998–1001.
36 J. H. van Esch, *Langmuir*, 2009, **25**, 8392–8394.
37 W. Xi, T. F. Scott, C. J. Kloxin and C. N. Bowman, *Adv. Funct. Mater.*, 2014, **24**, 2572–2590.
38 W. Tang and M. L. Becker, *Chem. Soc. Rev.*, 2014, **43**, 7013–7039.
39 J. Voskuhl, M. C. A. Stuart and B. J. Ravoo, *Chem. – Eur. J.*, 2010, **16**, 2790–2796.
40 R. Shimonkevitz, S. Colon, J. W. Kappler, P. Marrack and H. M. Grey, *J. Immunol.*, 1984, **133**, 2067–2074.
41 J. Karttunen and N. Shastri, *Proc. Natl. Acad. Sci. U. S. A.*, 1991, **88**, 3972–3976.
42 K. L. Kiick, E. Saxon, D. A. Tirrell and C. R. Bertozzi, *Proc. Natl. Acad. Sci. U. S. A.*, 2002, **99**, 19–24.
43 K. L. Kiick and D. A. Tirrell, *Tetrahedron*, 2000, **56**, 9487–9493.
44 S. I. van Kasteren, H. B. Kramer, D. P. Gamblin and B. G. Davis, *Nat. Protoc.*, 2007, **2**, 3185–3194.
45 S. I. van Kasteren, H. B. Kramer, H. H. Jensen, S. J. Campbell, J. Kirkpatrick, N. J. Oldham, D. C. Anthony and B. G. Davis, *Nature*, 2007, **446**, 1105–1109.